# Metal Ion Interaction with Phosphorylated Tyrosine Analogue Monolayers on Gold

**Rodrigo M. Petoral, Jr., Fredrik Björefors, and Kajsa Uvdal***

*Division of Sensor Science and Molecular Physics, Department of Physics, Chemistry and Biology (IFM), Linköpings universitet, SE-581 83 Linköping, Sweden*

*Received: June 29, 2006; In Final Form: September 5, 2006*

Phosphorylated tyrosine analogue molecules (pTyr-PT) were assembled onto gold substrates, and the resulting monolayers were used for metal ion interaction studies. The monolayers were characterized by X-ray photoelectron spectroscopy (XPS), infrared reflection−absorption spectroscopy (IRAS), cyclic voltammetry (CV), and electrochemical impedance spectroscopy (EIS), both prior to and after exposure to metal ions. XPS verified the elemental composition of the molecular adsorbate and the presence of metal ions coordinated to the phosphate groups. Both the angle-dependent XPS and IRAS results were consistent with the change in the structural orientation of the pTyr-PT monolayer upon exposure to metal ions. The differential capacitance of the monolayers upon coordination of the metal ions was evaluated using EIS. These metal ions were found to significantly change the capacitance of the pTyr-PT monolayers in contrast to the nonphosphorylated tyrosine analogue (TPT). CV results showed reduced electrochemical blocking capabilities of the phosphorylated analogue monolayer when exposed to metal ions, supporting the change in the structure of the monolayer observed by XPS and IRAS. The largest change in the structure and interfacial capacitance was observed for aluminum ions, compared to calcium, magnesium, and chromium ions. This type of monolayer shows an excellent capability to coordinate metal ions and has a high potential for use as sensing layers in biochip applications to monitor the presence of metal ions.

## 1. Introduction

Metal ions play important roles in many biological systems, for example, in the biochemical reactions catalyzed by particular metal-containing enzymes. In the human body system, both depletion and excess of certain essential metal ions, for example, Cu(II) and Al(III), can lead to a number of diseases.[1,2] Metal ions also have a significant impact in the environment. Free aluminum ions are, for example, harmful to both plants and animals, and they exist as contaminants in soil and freshwater.[3] The aluminum ion ($Al^{3+}$) is a typical hard metal ion, and the most probable binding sites in biosystems are negatively charged oxygen donors such as carboxylates, phenolates, catecholates, and phosphates.[4] Also, catecholamines, which are richly found in brains, may have an important role in $Al^{3+}$ binding.[4] Phosphorylated peptides and proteins are also suggested to play a role in the accumulation of $Al^{3+}$ during the neuron degradation process as, for example, in Alzheimer disease.[4] Hence, it is important to monitor low concentrations of metal ions in drinking water and in body fluids, as well as in recipients in the ecosystem.

One attractive option for monitoring the level of metal ions is the use of chelating agents. The recognition, binding, and interaction of specific metal ions to particular ligands must be understood to realize this, and it brings about the design of molecular systems to work as metal ion-sensing elements. A possible sensor system can be achieved by immobilizing molecules on a solid support and incorporating functional groups that are able to recognize and attract metal ions. Several different functionalized self-assembled monolayers (SAMs) have been reported to serve as potential metal ion sensors. Reinhoudt et al.[5] and Bryce et al.[6] reported the incorporation of crown-ether groups into SAMs, while Echegoyen et al.[7] investigated SAMs of cyclic and acyclic polyethers. Several of these SAM-based molecular systems have been reviewed by Gooding et al.[8] An interesting system that inspired this work was the exploitation of amino acids[9,10] and oligopeptides[11−13] as recognition elements. A specific example is a Gly-Gly-His tripeptide covalently linked to an alkanethiol SAM-modified gold electrode for the electrochemical detection specific to copper ions.[13] Recently, phosphorylated amino acid residues present in a fragment of a designed protein domain have been reported to bind with $Tb^{3+}$.[14,15]

In this work, a phosphorylated tyrosine analogue self-assembled on gold has been used for metal ion interaction studies. The composition and molecular structure of the analogue, as prepared and exposed to metal ions, was characterized using X-ray photoelectron spectroscopy, infrared reflection−absorption spectroscopy, and cyclic voltammetry. Electrochemical impedance spectroscopy was further used to monitor the interaction of the metal ions with the adsorbates. The aim of this work was to relate possible structural and orientational changes of the monolayers to metal ion exposure and to investigate the chelating capabilities toward aluminum ions and other bio-relevant metal ions.

## 2. Experimental Methods

**Assembly.** The phosphorylated tyrosine-terminated propanethiol (pTyr-PT), with chemical structure shown in Figure 1, was synthesized according to our previous work,[16] and initially having $Na^+$ as counterions. A 1 mM ethanol-based solution of pTyr-PT was used to incubate cleaned gold substrates for at least 24 h. A detailed description of the gold preparation, cleaning, and molecular assembly procedure can be found elsewhere.[17] After this step, the surfaces were ultrasonicated in

* Corresponding author. Fax: +46-13-288-969. E-mail: kaj@ifm.liu.se.

10.1021/jp064075m CCC: $33.50 
Published on Web 10/28/2006

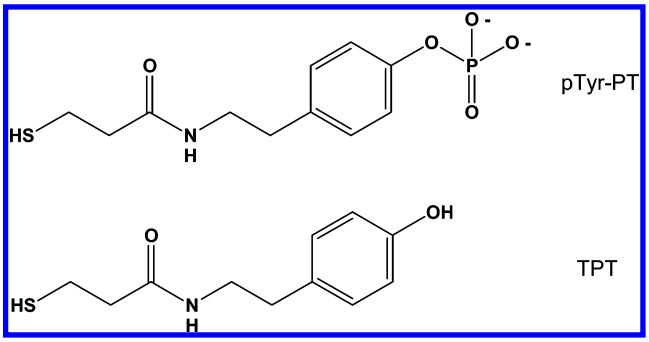


**Figure 1.** Chemical structure of phosphorylated tyrosine-terminated propanethiol (pTyr-PT) and tyrosine-terminated propanethiol (TPT).

ethanol for 10 minutes. The surfaces were then immersed in a solution of 0.1 M acetyl chloride in ethanol for one minute to exchange the sodium ions. This procedure also ensured that formation of bilayers or presence of physisorbed layers was avoided (further information can be found under Results and Discussion). The surfaces were then again ultrasonicated in ethanol for five minutes, dried in a stream of nitrogen, and immediately analyzed or exposed to metal ions.

Monolayers of nonphosphorylated tyrosine-terminated propanethiol (TPT), illustrated in Figure 1, were also prepared for comparison. Here, clean gold substrates were incubated in a 1 mM basic aqueous solution (MilliQ, 18.2 MΩ) of TPT (pH was adjusted to pH 12 using 1 M NaOH) for at least 24 h. The surfaces were then sonicated in water (also adjusted to pH 12) for five minutes, followed by blow-drying with nitrogen gas, and immediately analyzed or exposed to metal ions. The structure of the monolayers based on the basic aqueous solution of TPT was very similar to that of the monolayers formed using an ethanolic solution,[16,17] and hence not reported in this paper.

**Metal Ion Exposure.** The following procedure was done to expose the pTyr-PT adsorbates to different metal ions prior to XPS, IRAS, and CV analysis. To expose the monolayers to sodium, magnesium, or aluminum ions, 10 mM aqueous solutions of sodium hydroxide (NaOH, Merck), magnesium chloride hexahydrate ($MgCl_2 \cdot 6H_2O$, Merck), and aluminum nitrate nonahydrate ($Al(NO_3)_3 \cdot 9H_2O$, Kebo, Germany) were used, respectively (the pH values in the latter two solutions were 6−7). After 30 min, the surfaces were rinsed in water and dried under a stream of nitrogen.

**Ellipsometry.** Single-wavelength ellipsometry was performed using an automatic Rudolf Research AutoEL ellipsometer with a He−Ne laser light source, $\lambda = 632.8$ nm, at an angle of incidence of 70°. Freshly cleaned gold sample substrates were measured prior to incubation, and the collected refractive indices were later used in a model "ambient/organic film/gold", assuming an isotropic, transparent organic layer with the refractive index of $n = 1.5$. The film thickness was calculated as an average of measurements from five different spots on each sample.

**XPS.** XPS analyses were performed in a VG instrument with a CLAM2 analyzer and a twin Mg/Al anode. The base pressure in the analysis chamber was in the midrange of $10^{-10}$ mbar. The measurements were carried out with unmonochromated Al Kα photons (1486.6 eV), except for the sodium-treated surfaces, which used Mg Kα photons (1253.6 eV). The resolution was determined from the full width at half-maximum (fwhm) of the Au ($4f_{7/2}$) line, which was 1.3 eV with pass energy of 50 eV. The power of the X-ray source was kept constant at 300 W. The binding energy scale was aligned through the C (1s) peak at 284.6 eV. Measurements were made using photoelectron takeoff angles (TOA) of 30° and 80° with respect to the surface normal of the sample. The VGX900 data analysis software was used to calculate elemental composition from the peak areas and to analyze the peak positions. The adsorbates were measured at about 200 K except for the multilayer sample and monolayers treated with sodium ions, which were analyzed at room temperature.

**IRAS.** IRAS measurements were performed on a Bruker IFS66 Fourier transform spectrometer equipped with a grazing angle of incidence reflection accessory aligned at 85°. The infrared radiation was polarized parallel to the plane of incidence. Interferograms were apodized with a three-term Black−Harris function before Fourier transformation. The spectra were recorded by averaging 2000 interferograms at 4 $cm^{-1}$ resolution, using a liquid nitrogen-cooled mercury cadmium telluride (MCT) detector. The measurement chamber was continuously purged with nitrogen gas during the measurement.

**CV and EIS.** The cyclic voltammograms and impedance data were obtained with an Autolab PGSTAT 20 (EcoChemie, Utrecht, The Netherlands), equipped with a FRA2 frequency response analyzer unit. An Ag/AgCl-electrode served as the reference electrode, while a platinum wire acted as the counter electrode. Details of the electrochemical setup are described elsewhere.[18] The redox species used was 1.0 mM $K_3Fe^{III}(CN)_6$ (Merck) in either 100 mM $KNO_3$ (Merck) or 100 mM NaCl (Merck). The cyclic voltammograms were recorded between −0.30 and +0.60 V (vs Ag/AgCl) at a scan rate of 10 mV/s. The impedance data were obtained in either 100 mM $KNO_3$ or 100 mM NaCl at 21 logarithmically distributed frequencies in the range 200 Hz−2 kHz. The rms amplitude was 5 mV, and the DC potential was 0.0 V (vs Ag/AgCl). The differential capacitance was obtained by fitting the impedance data to an equivalent *RC* circuit, where *R* represents the solution resistance in series with the differential capacitance *C*. To compensate for nonideal behavior (for example, due to surface roughness), the capacitance was evaluated as a constant phase element (CPE).[19] The resulting power *n* for the present monolayers were in the range $n = 0.95-0.97$ ($n = 1$ for an ideal capacitor).

Prior to all measurements, the pTyr-PT-coated electrodes were immersed in 1 mM EDTA (prepared in either 100 mM $KNO_3$ or 100 mM NaCl) in order to remove any coordinated contaminants. Addition of an appropriate volume of metal ion solution was made to an electrolyte solution of 30 mL followed by manual stirring. The metal salts were $MgCl_2 \cdot 6H_2O$, $CaCl_2 \cdot 6H_2O$ (Merck), $Cr(NO_3)_3 \cdot 9H_2O$ (BDH Chemicals Ltd, England), and $Al(NO_3)_3 \cdot 9H_2O$.

## 3. Results and Discussion

The quality of the adsorbate by means of binding strength to the substrate, composition, thickness, and molecular orientation is of main importance for the function of the system as a metal ion chelator. In the following, we present an analysis of the quality of the adsorbates prior to and after metal ion exposure using XPS, IRAS, and CV. Detection of metal ion coordination was done using electrochemical impedance spectroscopy.

**Elemental Composition and Molecular Orientation of Phosphorylated Tyrosine Analogue prior to and after Metal Ion Exposure.** Null ellipsometry was used to verify the monolayer formation of the pTyr-PT on gold and to check the thickness of the adsorbate. It was found that the thickness of the adsorbate was 18.8 ± 0.3 Å, indicating a monolayer formation on the gold surface which is consistent with the expected value from molecular modeling. Physisorbed molecules

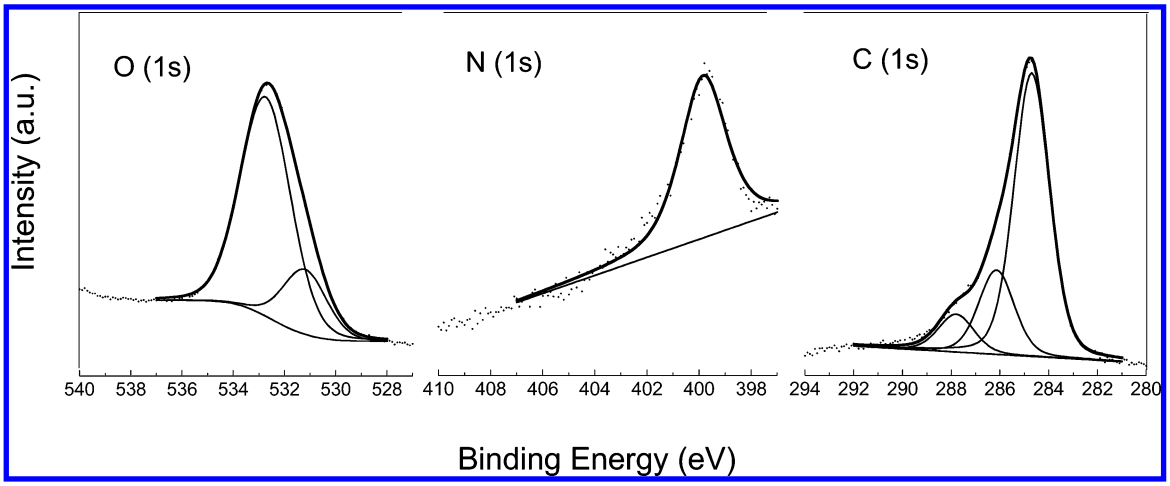


**Figure 2.** C (1s), N (1s), and O (1s) XP core-level spectra of the pTyr-PT monolayer on gold (unexposed to metal ions).

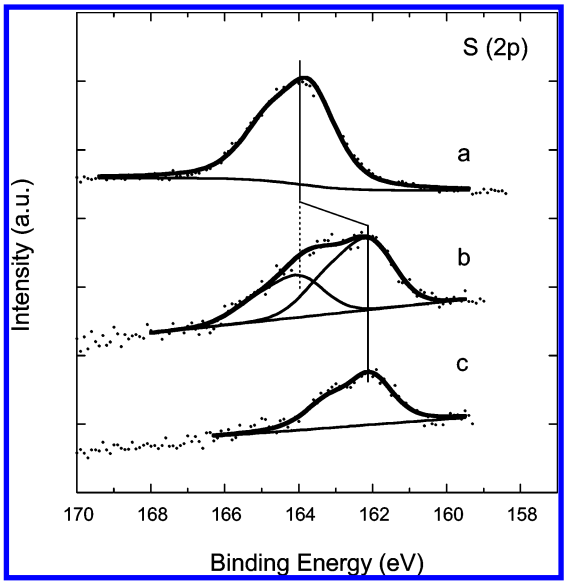


**Figure 3.** S (2p) XPS core-level spectra of the pTyr-PT molecule: (a) multilayer and monolayer, (b) prior to and (c) after treatment with acetyl chloride, on gold measured in bulk-sensitive mode (TOA = 30°).

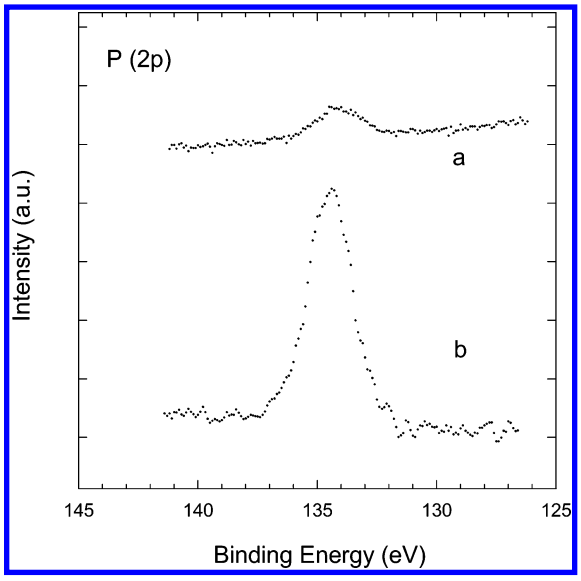


**Figure 4.** P (2p) XPS core-level spectra of the pTyr-PT molecule (not exposed to metal ions) adsorbed on gold measured in (a) bulk-sensitive mode (TOA = 30°) and in (b) surface-sensitive mode (TOA = 80°).

on top of the monolayer were obtained if the incubated surfaces were not treated with acetyl chloride, that is, the thickness was then determined to be 24.6 ± 0.6 Å. Aside from the removal of physisorbed molecules, acetyl chloride treatment replaces the sodium ions with protons from the acid, leaving the monolayer essentially free of metal ions. Removal of the physisorbed molecules with the aid of acetyl chloride will also be discussed below.

XPS is a surface-sensitive technique where information such as the composition, molecular binding strength, and orientation of an adsorbate can be extracted. Representative C (1s), N (1s), and O (1s) XP spectra of pTyr-PT not exposed to metal ions are shown in Figure 2. The S (2p) spectra of multilayer and monolayers, untreated and treated with acetyl chloride, respectively, are shown in Figure 3. The P (2p) spectra of an acetyl chloride-treated pTyr-PT are shown in Figure 4, while the XP core-level survey spectrum of the adsorbates (with the presence of $Al^{3+}$) is shown in Figure 5. The relative intensity ratios extracted from the XPS measurements are summarized in Table 1.

The C (1s), O (1s), and N (1s) spectra shown in Figure 2 are in good agreement with an earlier publication.[16] Here, a summary is given. The binding energy values of the elements found in the multilayer and monolayer assemblies of the phosphorylated tyrosine analogue are in agreement with the expected binding energy of the chemical species present in the molecule. The relatively broad C (1s) main peak at about 285 eV consists of several components assigned to the aromatic carbon component and aliphatic carbons. The curve-fitted peak at about 286 eV is assigned to carbons with sulfur or nitrogen as nearest neighbor, while the shoulder at about 288 eV is assigned to the carbon with oxygen as the nearest neighbor. The two O (1s) binding energy peaks are correlated to the carbonyl oxygen in the amide bond and the oxygen species present in the phosphate group. Water contribution, including the water coordinated to the metal ions, is observed as a broadening on the higher-binding-energy peak position (~533 eV) in the O (1s) spectrum of adsorbates, as expected. The N (1s) binding energy peak is positioned at about 399.5 eV, which is consistent with molecules having amide functionality. The observed S (2p) binding energy peak positioned at 163.7 eV for the multilayer spectrum shown in Figure 3a consists of a spin-orbit-split doublet, S ($2p_{1/2}$) and S ($2p_{3/2}$), representing one type of chemical state corresponding to the thiol group (−SH) commonly found in organosulfurs and alkylthiols.[16,17,20,21] The fitted S (2p) curve has a spin-orbit-split of 1.2 eV. For the monolayers in Figure 3b,c, the peak at 162 eV corresponds

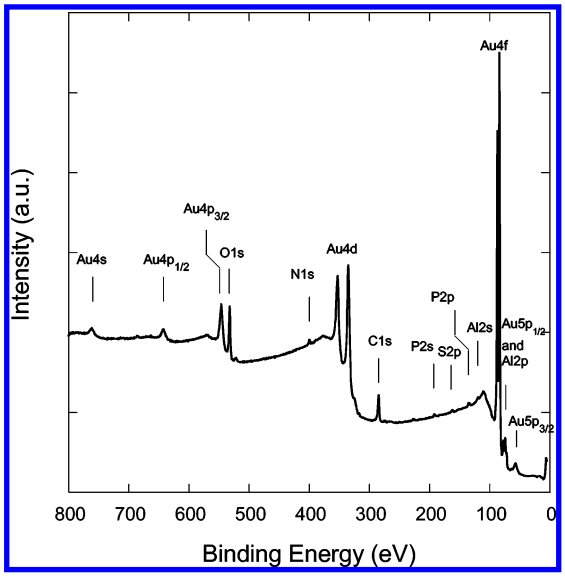


**Figure 5.** Survey XPS core-level spectrum of the pTyr-PT monolayer exposed to aluminum ions.

**TABLE 1: Relative Intensity Ratios of pTyr-PT Molecule on Gold**

| | relative intensity ratio | | | | | | |
|---|---|---|---|---|---|---|---|
| | P/C | P/O | P/N | P/S | P/Na | P/Mg | P/Al |
| stoichiometric ratio | (0.09) | (0.20) | (1) | (1) | (0.5) | (1) | (1.5) |
| multilayer | 0.08 | 0.24 | 1.35 | 1.23 | 2.37 | | |
| monolayer | | | | | | | |
| bulk mode | 0.16 | 0.24 | 1.82 | 2.89 | | | |
| surface mode | 0.18 | 0.27 | 2.40 | 4.80 | | | |
| 1. $Na^+$ exposed | | | | | | | |
| bulk mode | 0.08 | 0.21 | 1.46 | 1.84 | 2.75 | | |
| surface mode | 0.12 | 0.23 | 2.52 | 4.26 | 8.13 | | |
| 2. $Mg^{2+}$ exposed | | | | | | | |
| bulk mode | 0.09 | 0.16 | 1.13 | 1.86 | | 1.00 | |
| surface mode | 0.14 | 0.18 | 1.72 | 4.09 | | 4.12 | |
| 3. $Al^{3+}$ exposed | | | | | | | |
| bulk mode | 0.10 | 0.15 | 1.22 | 2.10 | | | 1.61 |
| surface mode | 0.11 | 0.13 | 1.66 | 2.72 | | | 2.00 |

to the sulfur chemisorbed to the gold surface.[16,17,20,21] It is interesting to note that the spectrum of the monolayers prior to acetyl chloride treatment has a peak at 164 eV, which is correlated to physisorbed molecules (Figure 3b), as compared to the treated one shown in Figure 3c. In addition, no trace of the peak associated with $Na^+$ is observed on the survey spectra of the monolayer (not shown). The peak at about 134 eV in the P (2p) spectrum of both multilayer and monolayers reveals the presence of the phosphate group.[22] The P (2p) spectra measured for a monolayer surface not exposed to metal ions are shown in Figure 4. For the multilayer film of pTyr-PT, the expected sodium ions are observed with XPS (figure not shown). Appearance of the expected metal ion was observed from the XPS survey spectra, measured for the different metal ion exposures. A proof of exchange of the expected cations ($Na^+$, $Mg^{2+}$, or $Al^{3+}$) was observed in the XPS spectra, and no trace of the anions ($Cl^-$, $NO_3^-$) was detected. An example of a survey spectrum of the adsorbate, with the presence of $Al^{3+}$, is shown in Figure 5.

The relative intensity ratio of the multilayer, shown in Table 1, reflects the composition of the pristine material. The P/C ratio of the monolayers also includes orientation effects (for further discussion see next paragraph). Excellent agreement with stoichiometric ratios was observed for the pTyr-PT monolayer, and also after exposure to $Mg^{2+}$ and $Al^{3+}$. Presence of extra coordinated water from $Mg(H_2O)_6^{2+}$ and $Al(H_2O)_9^{3+}$ could be a reason for the relatively low P/O ratio observed for monolayers with metal ions.

Angle-dependent XPS (XPS($\theta$)) results give an estimate on how the monolayers are oriented on the gold substrate. A monolayer not exposed to metal ions is suggested to have the phosphate groups oriented above the amide functionality and consequently above the chemisorbed thiol moiety. This is indicated by the relative increase of the P/N and P/S ratios from the bulk- to surface-sensitive mode. A relative increase (from bulk mode to surface mode) in the P (2p) peak intensity of monolayers prior to metal ion exposure was observed as shown in Figure 4, where the two peak intensities were normalized to the corresponding Au (4f) intensities. Increase of the P/N and P/S ratios was also observed for $Na^+$- or $Mg^{2+}$-exposed monolayers. Interestingly, for the monolayer exposed to $Al^{3+}$, no significant increase in the P/N and P/S ratios was observed as compared to the $Na^+$- and $Mg^{2+}$-exposed surfaces. This indicates a more compact orientation of the monolayers where the phosphate groups are oriented close to the chemisorbed sulfur atoms. Thus, an indication of a change in the monolayer structure/orientation can be inferred upon coordination of aluminum ions to the monolayer.

The amount of metal ions coordinated to the monolayer via the phosphate groups is reflected in the ratio of the P (2p) signal to the metal ion [Na (1s), Mg (2p), and Al (2s)] signal. Assuming that only electrostatic interaction occurs between the positively charged metal ions and the negatively charged phosphate groups, the expected ratios P/Na, P/Mg, and P/Al would be 1:2, 1:1, and 3:2, respectively. The result of the XPS measurements (in the bulk mode) showed that P/Na is almost five times higher than the expected value, while the P/Mg and P/Al values match the expected value. The discrepancy observed for the sodium-containing monolayer indicates that fewer metal ions are coordinated to the monolayer. A rapid decrease in the sodium signal was observed during the measurement, which most likely was related to the fact that the monolayer was analyzed at room temperature. The high-energy X-ray may have influenced the interaction between the sodium ions and the phosphate groups. Consequently, the remaining samples were analyzed at about 200 K.

IRAS is another complementary surface-sensitive technique to study the structure and orientation of molecular adsorbates on metal substrates by probing the IR-active vibrational modes. The reflection−absorption spectra for pTyr-PT adsorbates on gold with coordinated metal ions are shown in Figure 6. Important peaks are indicated in the figure, and all peak assignments were based on a previous study of the same molecules exposed to different counterions.[16] The peak at about 1650 $cm^{-1}$ is assigned to amide I (C═O symmetric stretch mode), and this is weak as compared to the peak in the transmission spectrum of a pTyr-PT (figure not shown). Due to the surface dipole selection rule,[23] it can be suggested that the main component of the transition dipole moments of the amide I stretch (oriented parallel to the C═O bond) is aligned nearly parallel to the gold surface. Amide II stretch (combination of H−N−C in-plane bend and C−N stretch) can be found as a peak at about 1550 $cm^{-1}$ and is enhanced compared to the transmission IR spectrum, indicating that this vibrational mode is oriented perpendicular to the surface. The behavior of the peaks corresponding to amide I and II vibrations is consistent with the orientation of the amide group having both C═O bond and N−H bond almost parallel to the gold surface. Ring vibrations are found at about 1611 and 1516 $cm^{-1}$, while the

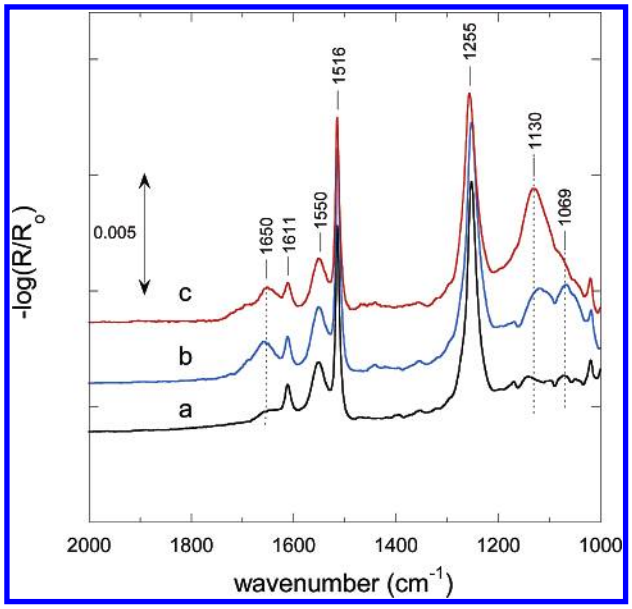


**Figure 6.** IRAS spectra of the pTyr-PT adsorbates on gold (a) prior to exposure to (b) $Mg^{2+}$, or (c) $Al^{3+}$.

P═O stretching modes (specifically the Ar:P−O−C stretching mode) are assigned at about 1255 $cm^{-1}$. Both ring and phosphate modes are strongly enhanced, suggesting a molecular orientation with the plane of the ring perpendicular to the surface. This observation is consistent with previous studies on the same molecule.[16,22] The effect of the presence of metal ions is reflected on absorption peaks at about 1130 and 1069 $cm^{-1}$. A significant increase in the intensity of these peaks can be observed as magnesium or aluminum is introduced. These peaks are ascribed to P−O stretch as the phosphates coordinate the metal ions. A similar trend was observed earlier when calcium or magnesium ions coordinated to phosphorylated serine analogues.[24] Another significant observation is a slight change in intensity at about 1650 $cm^{-1}$ (amide I) when either aluminum or magnesium ions are coordinated. This is interpreted as a reorientation of the pTyr-PT molecules to accommodate the counterions. This change in structure upon metal ion incorporation is also observed from the angle-dependent XPS results discussed earlier.

**Interfacial Capacitance and Electrochemical Blocking Properties of pTyr-PT Monolayers upon Interaction with Metal Ions.** To evaluate the coordination of metal ions with the adsorbates in a liquid environment, electrochemical techniques were employed. XPS and IRAS verified that metal ions could interact with the phosphate groups, and they also indicated a resulting change in the monolayer structure. With EIS, it is possible to investigate the metal ion interaction by evaluation of the interfacial capacitance, while CV offers structural information on the basis of the blocking of faradaic reactions.

The differential capacitance was evaluated by using frequencies between 2 kHz and 200 Hz, at a DC level of 0.0 V vs Ag/AgCl (in order to minimize influence from faradaic reactions). In this fairly small frequency range a series *RC*-circuit, where *R* represents the solution resistance and *C* the differential capacitance, is sufficient to model the impedance data.[24] To evaluate the possible use of these monolayers in sensor applications, the capacitance was measured after consecutive additions of metal ions in the concentration range of 1.0 $\mu$M−2.0 mM. In Figure 7, the capacitance as a function of the concentration of aluminum, chromium, calcium, and magnesium ions is displayed. The main explanation for the drop in

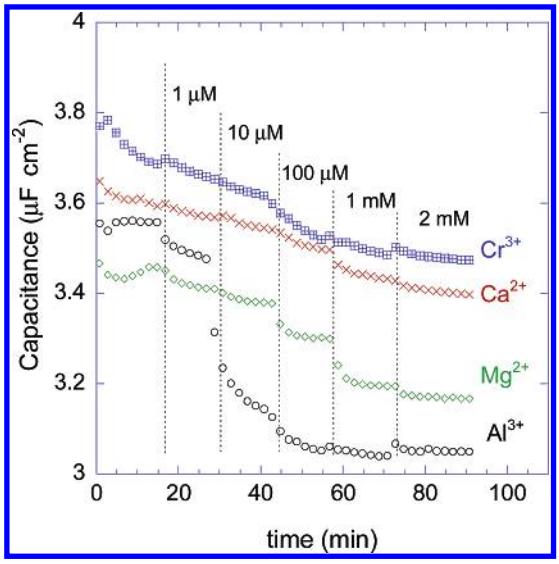


**Figure 7.** The differential capacitance of the pTyr-PT monolayer at increasing concentrations of metal ions.

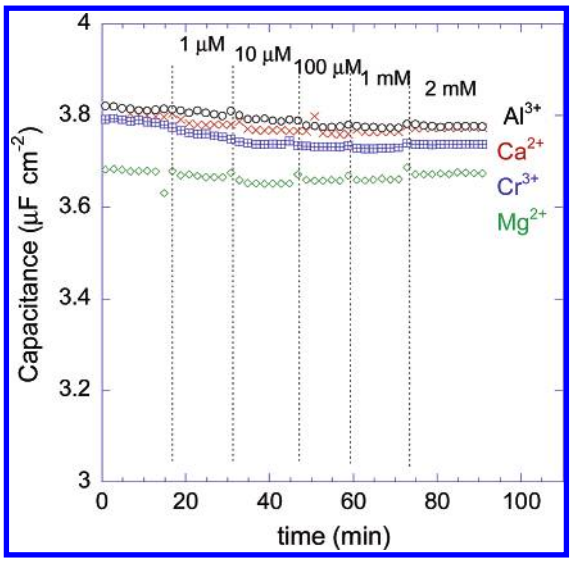


**Figure 8.** The differential capacitance of the TPT monolayer at increasing concentrations of metal ions.

capacitance is the decrease in the charge and/or polarity of the phosphate groups due to the coordination of metal ions.[24] As expected, no significant drop in the capacitance was obtained for the TPT monolayers after addition of metal ions in the same concentration range (see Figure 8), that is, metal ions cannot coordinate to the hydroxyl groups. The largest drop in capacitance, and also the lowest absolute value, was observed for aluminum ions, that is, the capacitance dropped from 3.56 to 3.05 $\mu$F $cm^{-2}$ after additions corresponding to a final concentration of 100 $\mu$M. At higher concentrations the capacitance was not significantly changed, which was probably due to saturation of the phosphate groups. The larger change in the capacitance observed for aluminum could be interpreted as a stronger ability to coordinate to the phosphate groups. Magnesium ions have, compared to calcium ions, likewise previously been found to coordinate more strongly to another phosphorylated amino acid derivative, that is, a phosphorylated serine analogue.[24] Interestingly, when comparing chromium and aluminum ions, the ionic charge is the same and the ionic radii are similar (67 pm and 75 pm, respectively[25]) however, the influence from the chromium ions on the capacitance was significantly smaller. We are, at present, improving our EIS experiments and equivalent

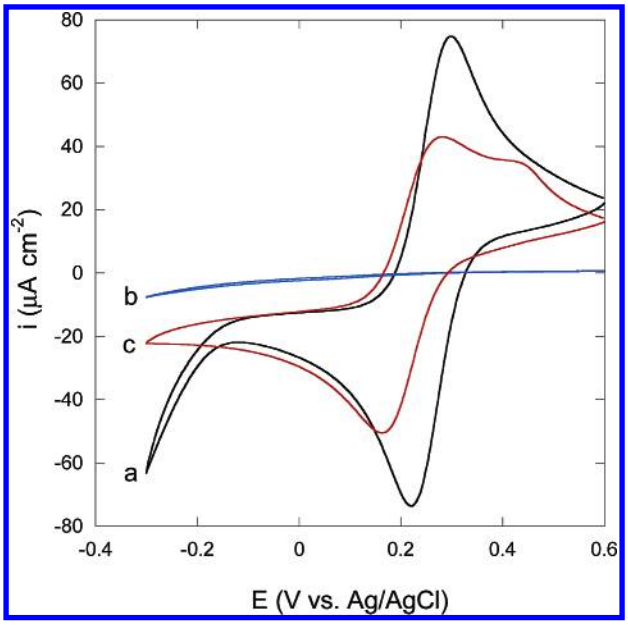


**Figure 9.** Cyclic voltammograms of (a) bare gold electrode, (b) pTyr-PT monolayer, and (c) pTyr-PT monolayer exposed to aluminum ions. All experiments in 1.0 mM $K_3Fe^{III}(CN)_6$ and 100 mM $KNO_3$ using a scan rate of 10 mV/s.

circuits in order to understand how the differential capacitance also is influenced by structural changes in the monolayer, in addition to the decrease in charge and/or polarity of the phosphate groups.

As is also obvious from Figure 7, the initial capacitances for the pTyr-PT monolayers were not exactly the same prior to addition of metal ions. This has previously been found to be related to exposure to contamination of metal ions, which also explains why the spread in the initial capacitances for the TPT monolayers in Figure 8 were smaller. In the previous study, it was also found that immersing the phosphate surfaces in an EDTA solution before use decreased the spread to some extent. To also determine the surface-to-surface uncertainty after addition of metal ions, eight electrodes with pTyr-PT monolayers were evaluated using an aluminum ion concentration of 1.0 mM. In this case, the differential capacitance (with 95% confidence limits) was found to be $3.11 \pm 0.06\ \mu F\ cm^{-2}$. The concentration dependence in Figure 7 indicates a possible use of the pTyr-PT monolayers for metal ion determinations, with a detection limit in the order of $1-5\ \mu M$. The poor selectivity toward common metal ions is, however, a drawback.

On the basis of the suppression of faradaic reactions, CV gives qualitative information on the blocking characteristics of molecular films. To confirm the structural changes observed with XPS and IRAS, voltammograms were recorded for a pTyr-PT monolayer before and after exposure to aluminum ions. Although quantitative data on blocking characteristics are difficult to extract from the voltammogram, the blocking properties of the pTyr-PT monolayers before the addition of aluminum ions were found to be fairly good (Figure 9b). This conclusion is mainly based on the very small faradaic current at and near the formal potential. This is somewhat surprising considering the complexity of the phosphorylated tyrosine functionality, which, compared to normal alkane chains, may restrict the organization on the surface. On the other hand, ring structures in similar thiols have previously been reported to have a certain degree of order in the monolayer.[17,21] The strength in this experiment is the comparison with the corresponding voltammogram after exposure to aluminum ions (Figure 9c). The latter indicates that the aluminum ions had a major influence on the blocking characteristics, that is, the ordering of the monolayers on the surface was severely affected. The shape of the resulting voltammogram was now found to be similar to the voltammogram obtained with a naked gold electrode (Figure 9a), and the absolute magnitude of the current was also comparable to the current for the naked gold electrode. The CV experiments hence support the findings from the spectroscopic experiments.

## 4. Conclusions

Phosphorylated tyrosine analogue molecules were assembled onto gold substrates followed by exposure to some different metal ions. To investigate the metal ion interaction, the surfaces were characterized by XPS, IRAS, CV, and EIS. XPS verified the presence of the expected metal ions in the monolayers, while coordination of metal ions to the phosphate groups was confirmed by both XPS($\theta$) and IRAS. The results also suggested a change in the structure/orientation of the monolayer when metal ions were introduced. Via CV, the structural change was detected by a reduced blocking capability of the monolayer. The largest change in structure and differential capacitance was observed when aluminum ions were coordinated to the monolayer.

The concept of using phosphorylated amino acid analogues for metal ion recognition applications is a promising approach. From an application point of view, it is important to also consider the structural changes of the chelating monolayer. We are, at present, also using other surface analysis and sensing techniques to be able to investigate the degree of selectivity of the monolayers to different metal ions. To mimic a real-life situation, a broader array of metal ions will be addressed in the future.

**Acknowledgment.** This project was supported by grants from the Swedish Research Council (Vetenskapsrådet) and The Carl Tryggers Foundation. R.M.P.J. was part of the Graduate School Forum Scientium, which was established by the Swedish Foundation for Strategic research (SSF). Johan Ekeroth and Andreas Carlsson are acknowledged for synthesizing the pTyr-PT and TPT molecules, respectively.

## References and Notes

(1) Theophanides, T.; Anastassopoulou, J. *Crit. Rev. Oncol. Heamatol.* **2002**, *42*, 57.
(2) Crapper, D. R.; Krishan, S. S.; Dalton, A. J. *Science* **1973**, *180*, 511.
(3) Martin, R. B. In *Aluminum in Chemistry, Biology and Medicine*; Nicolini, M., Zatta, P. F., Corain, B., Eds.; Cortina international: Verona, Raven Press: New York, 1991; Vol. 1.
(4) Rubuni, P.; Lakatos, A.; Champmartin, D.; Kiss, T. *Coord. Chem. Rev.* **2002**, *228*, 137.
(5) Flink, S.; van Veggel, F. C. J. M.; Reinhoudt, D. N. *J. Phys. Chem. B* **1999**, *103*, 6515.
(6) Moore, A. J.; Goldenberg, L. M.; Bryce, M. R.; Petty, M. C.; Monkman, P.; Marenco, C.; Yarwood, H.; Joyce, M. J.; Port, S. N. *Adv. Mater.* **1998**, *10*, 395.
(7) Herranz, M. A.; Colonna, B.; Echegoyen, L. *PNAS* **2002**, *99*, 5040.
(8) Gooding, J. J.; Mearns, F.; Yang, W.; Liu, J. *Electroanalysis* **2003**, *15*, 81.
(9) Liu, A. C.; Chen, D. C.; Lin, C. C.; Chou, H. H.; Chen, C. H. *Anal. Chem.* **1999**, *71*, 1549.
(10) Yang, W. R.; Gooding, J. J.; Hibbert, D. B. *J. Electroanal. Chem.* **2001**, *516*, 10.
(11) Torrado, A.; Walkup, G. K.; Imperiali, B. *J. Am. Chem. Soc.* **1998**, *120*, 609.
(12) Zeng, B. Z.; Ding, X. G.; Zhao, F. Q. *Electroanalysis* **2002**, *14*, 651.
(13) Yang, W. R.; Chow, E.; Willett, G. D.; Hibbert, D. B.; Gooding, J. J. *Analyst* **2003**, *128*, 712.

(14) Balakrishnan, S.; Zondlo, N. J. *J. Am. Chem. Soc*. **2006**, *128*, 5590.
(15) Liu, L. L.; Franz, K. J. *J. Am. Chem. Soc*. **2005**, *127*, 9662.
(16) Uvdal, K.; Ekeroth, J.; Konradsson, P.; Liedberg, B. *J. Colloid Interface Sci*. **2003**, *260*, 361.
(17) Petoral, R. M.; Uvdal, K. *J. Electron Spectrosc. Relat. Phenom*. **2003**, *128*, 159.
(18) Yang, Z.; Engquist, I.; Liedberg, B.; Kauffmann, J. M. *J. Electroanal. Chem*. **1997**, *430*, 189.
(19) Macdonald, J. R. *Impedance Spectroscopy*; Wiley: New York, 1987.
(20) Ishida, T.; Mizutani, W.; Akiba, U.; Umemura, K.; Inoue, A.; Choi, N.; Fujihira, M.; Tokumotu, H. *J. Phys. Chem. B* **1999**, *103*, 1686.
(21) Petoral, R. M.; Uvdal, K. *J. Phys. Chem. B* **2003**, *107*, 13396.
(22) Ekeroth, J.; Borgh, A.; Konradsson, P.; Liedberg, B. *J. Colloid Interface Sci*. **2002**, *254*, 322.
(23) Francis, S. A.; Ellison, A. H. *J. Opt. Soc. Am*. **1959**, *49*, 131.
(24) Ekeroth, J.; Konradsson, P.; Björefors, F.; Lundström, I.; Liedberg, B. *Anal. Chem*. **2002**, *74*, 1979.
(25) Shannon, R. D.; Prewitt, C. T. *Acta Crystallogr*. **1969**, *B25*, 925.